The dual-band NIKA: Technical Note 2 v1.0, IRAM run 2011,2012,2013

February 24, 2017

A. Monfardini, A. Benoit, M. Calvo, Institut Néel (IN) MCBT, BP 166, 38042 Grenoble, France,

F. X. Désert, N. Ponthieu, Institut de Planétologie et d'Astrophysique de Grenoble (IPAG), BP 53, 38041 Grenoble, France

A. Sievers, IRAM, Granada, Spain

Miscellaneous frequency and fits file information for the IRAM2011 run.

Note 2 is an enlarged version of Note 1 with 1D polynomial fit added, FXD 14 Jan 2014.

Chapter 1

Frequencies

Data acquisition rate is $f_{acq} = \frac{1.9\times10^3}{80} = 23.75$ Hz, hence one integration is 42.1053 ms.

To get the absolute frequency, Hz_per_bin= $\frac{498.074\times10^6}{2^{18}} = 1900.0015$ Hz .

If one uses the IDL routine read_camera_data, then the tone frequency of each kid is available in kHz as kidpar.kid_freq [Actually no, we must use a separate output for the routine] . Both 1 and 2 mm channels span a range of frequencies from 1.311 to 1.524 GHz.

The so-called $RfdIdQ$ (the first vector in the data for each kid) is the resonance central frequency in units of Hz starting at zero at the beginning of each scan (by construction). Thus, it is not the absolute frequency. One can work out how the tone frequency is different from the central resonance frequency by propagating from scan to scan the offsets obtained from the last frequency sweep scan. In more detail: I is the integration of 40 elementary measurements

$$I = \sum_{j=0}^{39} i_j \, ,$$

with one elemetary measurement acquired at 0.950 kHz. The modulation of the carrier frequency occurs with a step of 2 kHz at this rate of 0.950 kHz (the modulation period is thus 2.10526 ms). The measured dI is the difference between the integration of 20 measurements in the high frequency steps and the integration of the 20 measurements in the low frequency steps:

$$dI = \sum_{k=0}^{19} (i_{2k+1} - i_{2k})$$

So the derivative of I should be written as

$$\frac{\partial I}{\partial f} = 2\frac{dI}{2 \text{ kHz}} \, ,$$

and similarly for Q (beware with *YAFOT*, yet another factor of two). The $RfdIdQ$ is obtained by integrating the following formula:

$$\Delta RfdIdQ = \Delta f \, \frac{\Delta I. < dI > + \Delta Q. < dQ >}{< dI >^2 + < dQ >^2} \, ,$$

where Δ represents the difference of measurements between one sample and the previous sample and <> means that an average of the 100 values centered on the sample has been computed and Δf = 1 kHz. The averaging is done to limit the noise on the dI and dQ measurements. This has limitations (see below) for quickly varying signals.

Chapter 2

File Exchange format

TOI

Time ordered information (TOI) files containing the raw NIKA data or clean data should be exchanged between the parties (IRAM, IN, Cardiff, ...). We propose to stick to the format agreed with IRAM during the NIKA#3 October 2011 run. We can extend it if needed with flags and calibrations. Files are split by wavelength, so we generate 2 files per scan.

Primary header (extension 0) should contain a line stating the origin of the data:

TELESCOP= 'IRAM 30m' / Telescope Name

ORIGIN = 'IRAM ' / Organization or institution

DATE = '2012-01-21T09:31:01' / file creation date (YYYY-MM-DDThh:mm:ss UT)

INSRUME = 'NIKA2011_IRAMOct_2mm'

Other coment or keyword lines can indicate the processing used. For the present conversion I use the keyword N2I (NIKA to IRAM)

N2I = 'v8 ' / 'NIKA to IRAM conversion program version '

DATE = '2012-01-21T09:31:01' / file creation date (YYYY-MM-DDThh:mm:ss UT)

INTTIME = '0.0421053' / 'seconds per integration'

COMMENT raw data

Secondary header (extension 1) should contain one line stating the name of the extension and what is in the binary table in extension 1 *e.g.*:

'EXTNAME', 'RawData', 'MJD, Sample, Raw R, I, Q, dI, dQ'

The data themselves are written as the R column, then the I column, and so on. In one fits column, we have 150 detectors per line (150 columns) and the time samples increasing with the line number. Thus a 2D array is embedded in one fits column. MJD is a double. Sample in long integer. Data are single or double precision float. Flag column can be added as byte.

FPG

The focal plane geometry should be described in fits binary table files with the following format:

One line per detector. As many columns as needed. For example,

PixelNumber, Pixel_xindex, Pixel_yindex, x_arcsec, y_arcsec, FWHMmajor_arcsec, FWHMminor_arcsec, BeamAngle_degree

PixelNumber goes from 0 to 149 (one FPG file per channel). Pixel_[x, y]index is an integer giving the association of a given sky beam to a grid node. [x,y]_arcsec are the sky beam position in Nasmyth coordinates (i.e. after derotation from elevation). FWHM[major,minor]_arcsec is the beam FWHM of the elliptical Gaussian fit along with the beam orientation in degrees (anticlockwise from the x axis, TBC).

The header should contain the date and scan number from which the FPG has been deduced.

MAP

Maps can be written in the usual primary extension (0) as cubes (NAXIS1 and NAXIS2 should be the x and y map coordinates, NAXIS3 being the number of maps). The header should describe the meaning of NAXIS3 and how the maps are ordered (by scans, by detector, by [average, noise, weight] triplet, and so on.). They share the same projection system which is described in the primary header.

Chapter 3

2D polynomial fit

There are limitations to the on-line computation of the Response in frequency as shown in Chap.~1. The averaging by 100 points can produce hysteresis effect whereas we would like to go back to the same resonance frequency when the Kid is back to the same $I,\ Q$. We have a new formulation that involves 2D polynomial fitting of

$$F = P(I,\ Q)$$

where P is a polynomial of the two measured quantity and F is the resonance frequency to be found. The first derivative of that function yields the inverse of the $dI,\ dQ$ measurements. We minimize the quantity

$$A = \sum_t \left[\left(\frac{\partial F}{\partial I} - \frac{dI\ \Delta f}{dI^2 + dQ^2} \right)^2 + \left(\frac{\partial F}{\partial Q} - \frac{dQ\ \Delta f}{dI^2 + dQ^2} \right)^2 \right] (dI^2 + dQ^2)$$

for a given Kid and a given scan which yields the polynomial coefficients and thus the resonance frequency up to a constant.

The figures show that the obtained new frequency (in blue in the upper left panel) called Pf as a function of sample number is different in amplitude but usually closely follows the initial frequency measurement (black in the upper left panel) Rf (upper middle panel). The white noise is barely affected (upper right panel). Lower panels show the quality of the fit with a third-order polynomial (black dots are the measurements, blue diamonds are the results of the fit, contours represent constant value of the resonance frequency).

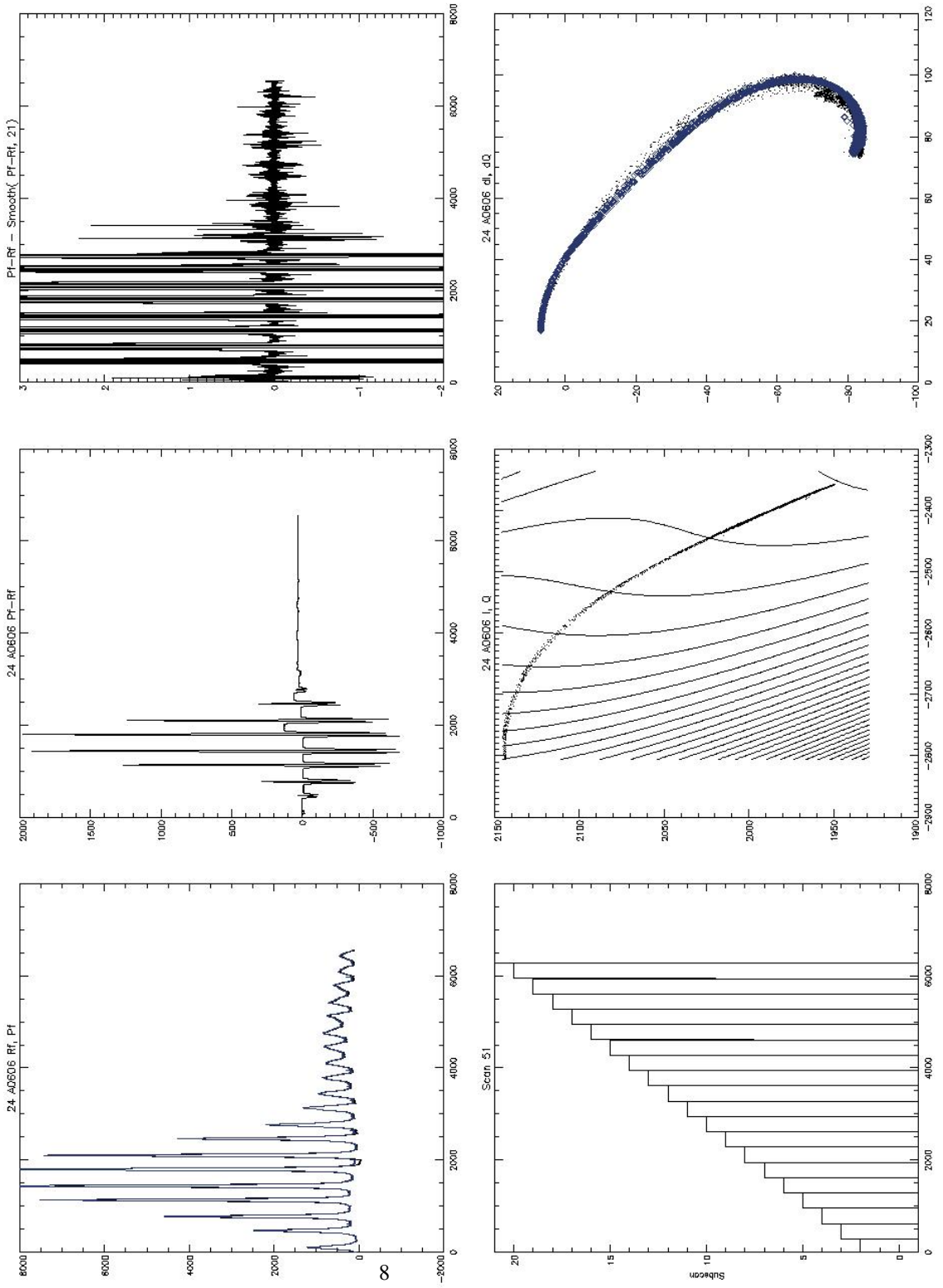

Figure 3.1: Polynomial fit to a scan on Mars for Kid 24

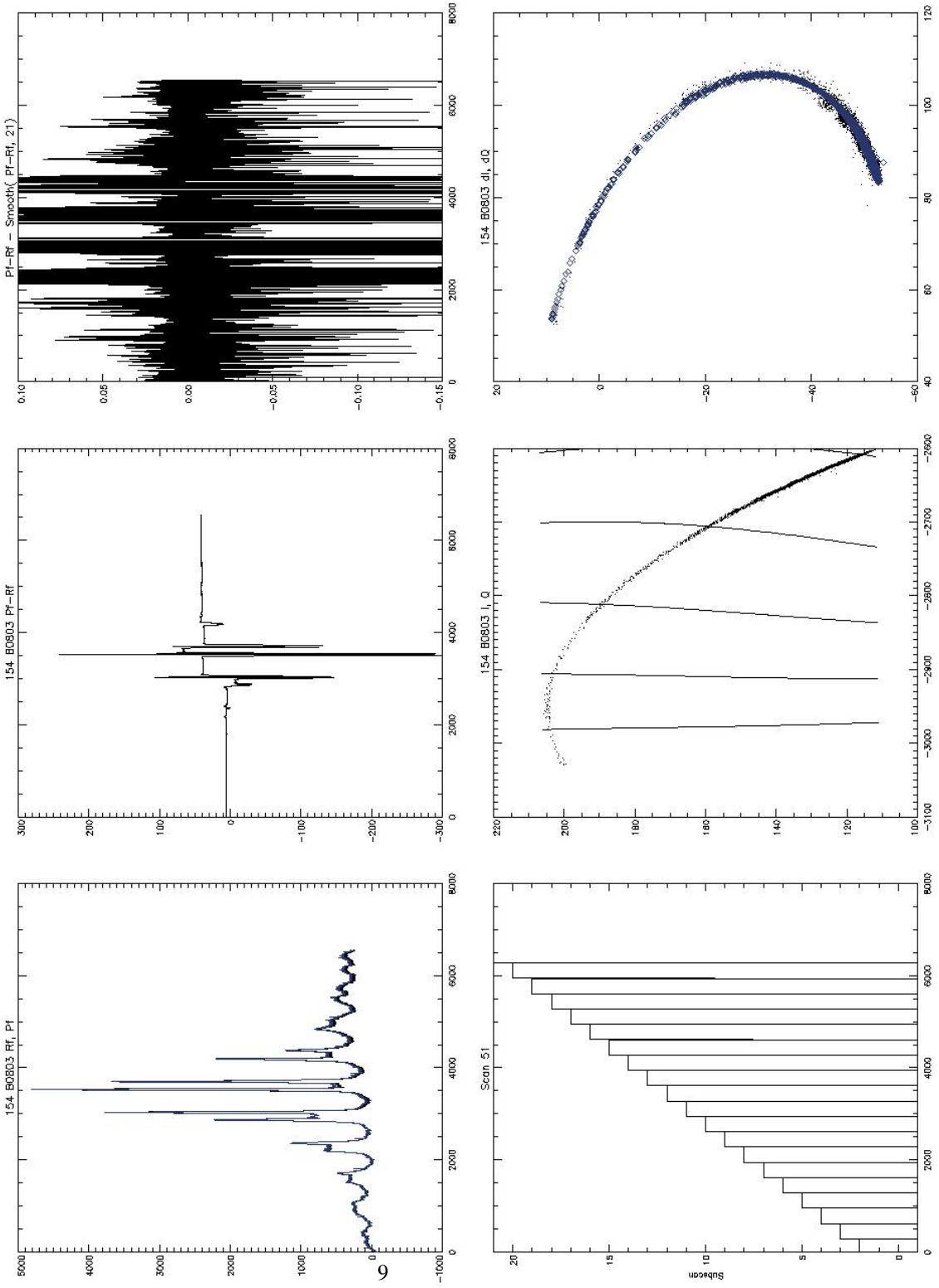

Figure 3.2: Polynomial fit to a scan on Mars for Kid 154

Chapter 4

New 1D polynomial fit

We show here a simplified version of the previous method. It relies on 1D polynomial fit which is more robust than the 2D version in principle. It is also easier to implement in terms of algorithms. The idea is to find how to "project" I,Q and dI, dQ onto an axis in a way as linear as possible with frequency (itself assumed linear with optical power). For that, we study the expected physical $Z = I + jQ$ complex dependency of a KID with frequency. G. J. Grabovskij, L. J. Swenson et al (arXiv:0809.4919) have shown that

$$Z = \frac{Z_r z_1}{Z_r z_2 + z_3} \tag{4.1}$$

where z_1, z_2 and z_3 are constant complexes, and $Z_r = \frac{1}{2} + j(f - f_0)/w$ where f_0 and w are constant real values in Hz. The location of Z is on a circle (at least approximately when near the resonance). The inverse of Z is a circle but we can normalize so as to have an infinite radius circle, which can be expected to be linear with the KID frequency. To simplify the solution of this inversion we proceed in two phases. The first phase is to scale, translate, rotate and reverse the initial circle so that it is identical to the reference circle which has $\frac{1}{2}$ radius and is centered on $(\frac{1}{2}, 0)$ in the complex plane, as defined by:

$$Z_{ref} = \frac{1}{2} + \frac{1}{2}\cos\phi + j\sin\phi = \cos\frac{\phi}{2}\exp j\frac{\phi}{2}$$

The second phase consists in inverting that reference circle, as $\frac{1}{Z_{ref}} = Z_{res}$

$$Z_{res} = \frac{1}{\cos\frac{\phi}{2}}\exp -j\frac{\phi}{2} = 1 - j\tan\frac{\phi}{2},$$

and $f = f_0 + \frac{w}{2}\tan\frac{\phi}{2}$. The imaginary part of the inversion of the reference circle is just linearly dependent on the frequency (assumption). To calibrate this dependency (because the linearity is only approximate) we must rely on the dI, and dQ measurements.

4.1 Circle fit

The first phase is best achieved with a circle fit to the data samples. If r is the radius of the circle and x_c, y_c its center and $\alpha = atan(\frac{y_c}{x_c})$, then Z becomes Z_{norm} with $I_{norm} = -\frac{1}{2r}[(I - x_c)cos\alpha + (Q - y_c)sin\alpha] + \frac{1}{2}$, and $Q_{norm} = \frac{1}{2r}[-(I - x_c)sin\alpha + (Q - y_c)cos\alpha]$. This is shown in Fig. 4.1 where the top-left plot shows Z and the top-right plot shows Z_{norm}. This figure is made with a simple simulation using Eq. 4.1 and including some noise. The bottom-left plot shows the inverse of Z_{norm}. The data points lie mostly along the imaginary line of abscissa 1 and of ordinate y_3.

4.2 1D polynomial fit

We need to calibrate y_3 which is in principle proportional to $f - f_0$. The modulation technique does that for us for the derivative function. Let us call dI, and dQ, the measured variations of the signal with a modulation of frequency of Δf. The normalized variations are $dI_{norm} = -\frac{1}{2r}[dIcos\alpha + dQsin\alpha]$, and $dQ_{norm} = \frac{1}{2r}[-dIsin\alpha + dQcos\alpha]$. The derivative of the inverse complex is $dZ_{res} = -dZ_{norm}/Z^2_{norm}$. We then take the imaginary part of that : dy_3 and use it to calibrate y_3 in this way: we fit $\frac{\Delta f}{dy_3} = R_n(y_3)$ where R_n is a polynomial function with a degree n (see bottom-right panel of Fig.. 4.1) which is easy to integrate into P_{n+1} (with $\dot{P}_{n+1} = R_n$). We then obtain the relative frequency of the kid from y_3 only with $f - f_0 = P_{n+1}(y_3)$ which is plotted in Fig. 4.2 along with the residual of the fit.

The method is robust if the polynomial fit is weighted. Indeed the noise on the derivative measurement ($\frac{\Delta f}{dy_3}$) increases as the phase changes (see the bottom-right panel of Fig. 4.1 where the flaring away from the zero phase is apparent). The noise is proportional to the noise in dy_3 divided by dy_3^2. The noise in dy_3 is not constant. It can be shown that it is inversely proportional to the distance of the current I,Q point to the point in the circle which is opposite to the resonance point. This noise model can also be used to show that the noise on the recovered frequency is flaring as we go away from the resonance. To a good approximation, the rms noise is proportional to $1 + tan^2\frac{\phi}{2} = 1 + (\frac{2(f-f_0)}{w})^2$.

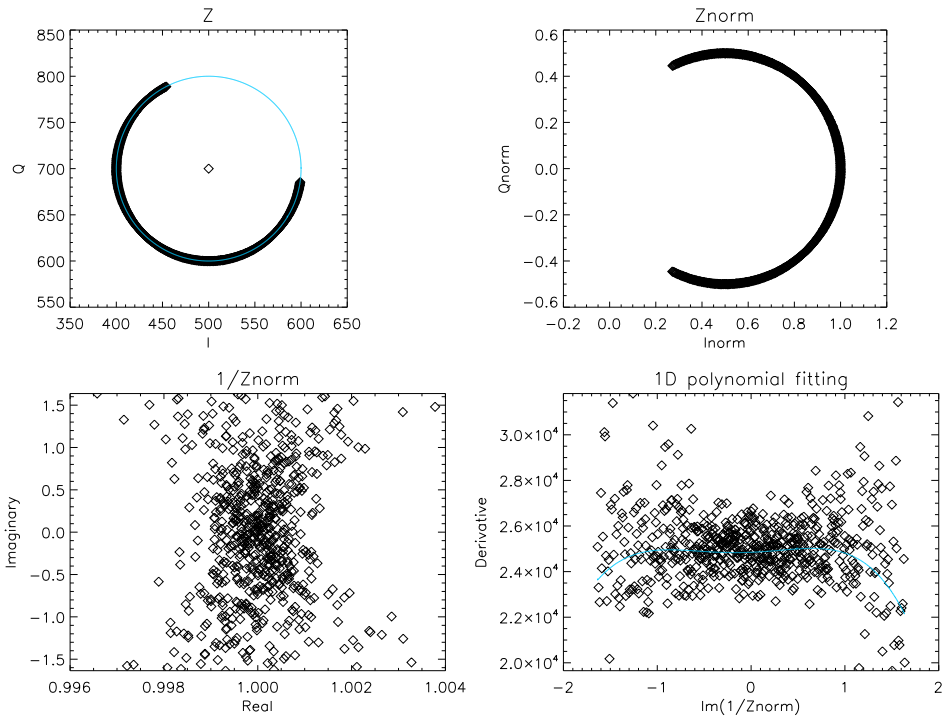

Figure 4.1: 1D Polynomial fit to a simulation of one KID. Top-left: diamonds are individual I, Q points on a circle (blue curve). Top-right: normalized circle transformation of the points into the reference circle coordinates. The resonance is reached at (1,0). Bottom-left: complex inverse of the points in the previous complex plane. Bottom-right: 1D polynomial fit (blue curve) to the derivative data points corresponding to dI, dQ normalized and inverted.

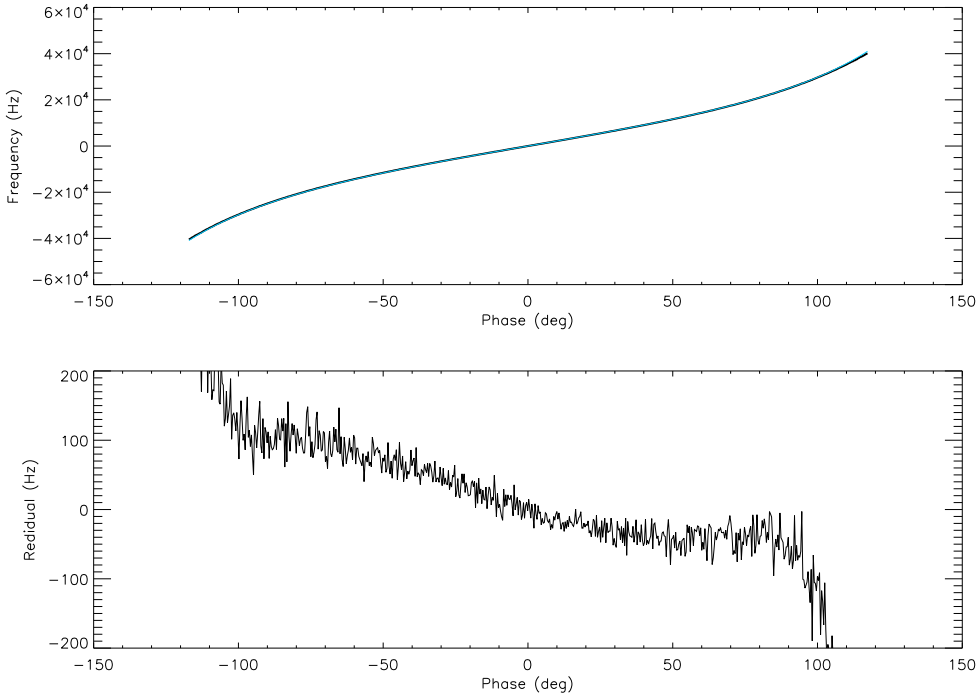

Figure 4.2: Comparison between the KID simulation and the 1D polynomial retrieval. Top plot: Relative KID frequency as a function of the phase ϕ in the circle as deduced from the 1D polynomial fit (black curve) and from the initial simulation (blue curve). Bottom plot: residual frequency (black curve minus blue curve) as a function of the same phase.